

# ChemComm

Accepted Manuscript



This is an *Accepted Manuscript*, which has been through the Royal Society of Chemistry peer review process and has been accepted for publication.

*Accepted Manuscripts* are published online shortly after acceptance, before technical editing, formatting and proof reading. Using this free service, authors can make their results available to the community, in citable form, before we publish the edited article. We will replace this *Accepted Manuscript* with the edited and formatted *Advance Article* as soon as it is available.

You can find more information about *Accepted Manuscripts* in the [Information for Authors](#).

Please note that technical editing may introduce minor changes to the text and/or graphics, which may alter content. The journal's standard [Terms & Conditions](#) and the [Ethical guidelines](#) still apply. In no event shall the Royal Society of Chemistry be held responsible for any errors or omissions in this *Accepted Manuscript* or any consequences arising from the use of any information it contains.

## COMMUNICATION

# Non-volatile Organic Transistor Memory Devices Using the Poly(4-vinylpyridine)-based Supramolecular Electrets

Cite this: DOI: 10.1039/x0xx00000x

Received 00th January 2012,  
Accepted 00th January 2012

Y.-H. Chou, Y.-C. Chiu, W.-Y. Lee, and W.-C. Chen\*

DOI: 10.1039/x0xx00000x

www.rsc.org/

**Supramolecular electrets consisted of poly(4-vinylpyridine) (P4VP) and conjugated molecules of phenol, 2-naphthol and 2-hydroxyanthracene were investigated for non-volatile transistor memory applications. The memory windows of these supramolecular electret devices were significantly enhanced with increasing the  $\pi$ -conjugation size of the molecule. An high ON/OFF current ratio of more than  $10^7$  over  $10^4$  s was achieved on the supramolecule based memory devices.**

Organic non-volatile memory (ONVM) devices have received extensive research interest recently due to the advantages of low cost and easy processing for flexible electronic applications,<sup>1</sup> such as radio frequency identification tags or flexible smart phones. Among various techniques for fabricating memory devices, the organic field-effect transistor (OFET) memory is an emerging and promising trend because of its non-destructive readout based on a easily integrated structure and multi-bit storage in a single transistor. The device configuration in OFET memory is a conventional transistors with an additional charge storage layer between the semiconductor layer and gate contact. The charge storage layer can be dielectric materials with a long-term charge storing ability or electrostatic polarization, including the chargeable polymer electret,<sup>2</sup> organic ferroelectric oriented-dipole dielectric materials,<sup>3</sup> donor-acceptor polyimides,<sup>4</sup> and nanoparticles (NPs)<sup>5</sup> or graphene oxide embedded gate dielectrics.<sup>6</sup> However, the above approach usually requires a complicated synthetic or hybridization procedures. Supramolecules are formed through complexation between an appropriate linear polymer and a small molecule using the non-covalent interaction, such as electrostatic interaction, hydrogen bonding, metal-ligand coordination bond,<sup>7</sup> to form a graft-copolymer-like structure. It could provide a facile way to prepare high performance non-volatile memory devices and omit the complicated processes of synthesis for new polymer electrets.

In this study, we construct supramolecules by attaching small molecule, including phenol, 2-naphthol, and 2-hydroxyanthracene, to the polymer (P4VP) side chains *via* hydrogen bonding. These three molecules contain a different pendant  $\pi$ -conjugated length (Fig. 1a)

and thus could be used to explore the effect of conjugated length on memory characteristics. The relationship between electrical properties and mechanism in the supramolecular dielectric was investigated. The formation of hydrogen bonds between the hydroxyl group of phenol and the pyridine nitrogen of P4VP was investigated by FTIR. Compared with pure P4VP, the FTIR result shows that the addition of phenol mainly affects the bands related to those stretching modes of pyridine ring at 1597 and 993  $\text{cm}^{-1}$  (Fig S1, *Supporting Information (SI)*). The pyridine bands at these two positions tend to shift to higher wavenumbers with increasing the molar ratio of 2-hydroxyanthracene, which is attributed to the pyridine complexed with the hydroxyl groups. The similar shifting is also observed in P4VP(phenol)<sub>x</sub> and P4VP(2-naphthol)<sub>x</sub>. We further estimate the fraction of pyridine groups of P4VP involved in the formation of hydrogen bonding (Fig. 1b). The fraction of hydrogen-bonded pyridines ( $f_{\text{OH-pyridine}}$ )<sup>7c</sup> is defined as

$$f_{\text{OH-pyridine}} = \frac{A_{1604}}{A_{1604} + A_{1597}}$$

where A is the peak area at 1604 or 1597  $\text{cm}^{-1}$  and the variation on the  $f_{\text{OH-pyridine}}$  value with the molar ratio x is shown in the Figure 1. The peak in the region of 1590–1610  $\text{cm}^{-1}$  can be divided into two peaks at 1597 and 1604  $\text{cm}^{-1}$  by deconvolution (Figure S1). The band at 1597  $\text{cm}^{-1}$  is characteristic of the P4VP-only sample (the bottom line in Figure S1e), indicating “free” pyridine. Apparently, a linear relationship is observed in the case of  $x \leq 0.5$  for P4VP(phenol)<sub>x</sub>, P4VP(2-naphthol)<sub>x</sub>, and P4VP(2-hydroxyanthracene)<sub>x</sub>. It indicates that the conjugated molecules are bound to the pyridine groups in P4VP chains with intermolecular hydrogen bonding. However, further increase of the molar ratio (> 0.5) leads to a nonlinear behaviour. This may be attributed to the steric hindrance from the bulky benzene rings of the molecules and suppress the formation of intermolecular hydrogen bonding. Thus, P4VP(phenol)<sub>1</sub>, P4VP(2-naphthol)<sub>1</sub>, and P4VP(2-hydroxyanthracene)<sub>1</sub> exhibit the maximum  $f_{\text{OH-pyridine}}$  of around 71%, 70% and 64%, respectively. This may be related to 2-Hydroxyanthracene with the most bulky benzene rings, thus leading to the lowest degree of hydrogen bonding. The molecular packing of

P4VP(phenol)<sub>1</sub>, P4VP(2-naphthol)<sub>1</sub>, and P4VP(2-hydroxyanthracene)<sub>1</sub> characterized by X-ray diffraction (Figure S2, *SI*) show The d-spacing values of 4.39, 4.43, and 4.69 Å, respectively. This suggests that the longer benzene moieties causes the stronger repulsion and leads to a larger d-spacing.

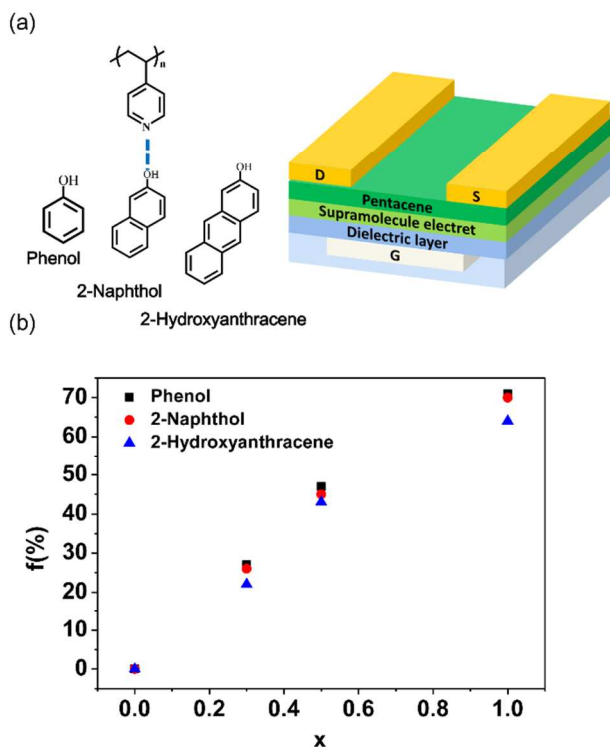


Fig. 1. (a) Chemical structure of supramolecule electrets and schematic configuration of the pentacene-based OFET memory device. (b) Variations of hydrogen-bonded pyridines (f) of P4VP(Phenol)<sub>x</sub>, P4VP(2-Naphthol)<sub>x</sub>, and P4VP(2-Hydroxyanthracene)<sub>x</sub> with mole ratio (x).

The electrical characteristics of P4VP(phenol)<sub>x</sub>, P4VP(2-Naphthol)<sub>x</sub>, and P4VP(2-hydroxyanthracene)<sub>x</sub> were evaluated using a bottom-gate/top-contact OFET configuration and *p*-type pentacene as a charge transport layer (Fig. 1a). The polymer electret film reveals a smooth surface with a small RMS roughness of 1.8-2.9 nm (Figure S3, *SI*). The transfer characteristics of the pentacene OFET devices with P4VP(2-Hydroxyanthracene)<sub>x</sub> as electrets are shown in Figure 2. These curves exhibit a typical *p*-type accumulation mode. The 300-nm-thick SiO<sub>2</sub> wafer has the capacitance of 10.9 nF/cm<sup>2</sup>. The supramolecular dielectric exhibits the capacitance of 8.3-8.7 nF/cm<sup>2</sup>. The saturation-regime field-effect mobility ( $\mu$ ) of the pentacene OFET using these supramolecule electrets are 0.1-0.2 cm<sup>2</sup>V<sup>-1</sup>s<sup>-1</sup>, as summarized in Table 1. The surface structure of pentacene on the supramolecular electrets was also characterized by AFM (Figure S4, *SI*). The pentacene crystals showed similar grain sizes of around 220-237nm on the supramolecular dielectrics surface. Even though changing the molar ratio of 2-hydroxyanthracene, the supramolecule dielectric layers showed similar roughness of 2.9-1.8 nm (Figure S4, *SI*). These surface structure analyses indicate that the morphology did not have a significant influence on the electrical memory behaviour and electrical properties.

To evaluate the electrical memory performance, the device was operated by applying appropriate gate pulse ( $\pm 100$ V) for one second to lead the shifts of the transfer curves. These gate pulses resulted in the different conducting states (high- (ON state) and low-conductance (OFF state) states) at zero gate bias conditions ( $V_g = 0$  V). When applying a positive gate bias ( $V_g = 100$  V for 1 s), the transfer curves were substantially shifted in the positive direction, served as the writing process, leading to a high drain current (ON state) at  $V_g = 0$  V. When applied a reverse gate bias ( $V_g = -100$  V for 1 s), the transfer curve was shifted to negative direction served as the erasing process. The shifting of the transfer curves through applying a writing and erasing gate bias is defined as the *memory window*. Figure 2 and shows the typical transfer curves of the OFET memory devices based on the pentacene thin film with P4VP(2-Hydroxyanthracene)<sub>1</sub>. The summary of the memory performance are shown in Table 1. P4VP(2-Hydroxyanthracene)<sub>1</sub>, P4VP(2-Hydroxyanthracene)<sub>0.5</sub> and P4VP(2-Hydroxyanthracene)<sub>0.3</sub> show the memory windows of 76, 61 and 52 V, respectively. Note that, the  $f_{OH-Pyridine}$  for P4VP(2-Hydroxyanthracene)<sub>1</sub>, P4VP(2-Hydroxyanthracene)<sub>0.5</sub> and P4VP(2-Hydroxyanthracene)<sub>0.3</sub> are 64, 43 and 22, respectively. This suggests that the memory window is enhanced with the increased fraction of the hydrogen bonding between hydroxyl groups and pyridines. In comparison, we prepared the pentacene-based device with 2-hydroxyanthracene as the electret (Figure S5d, *SI*). The pentacene devices made on the 2-hydroxyanthracene thin film exhibits a narrow memory window of 11 V. This limited charge trapping ability may be attributed to the strong  $\pi$ - $\pi$  interaction within 2-hydroxyanthracene, leading to the fast relaxation of the trapped charges.

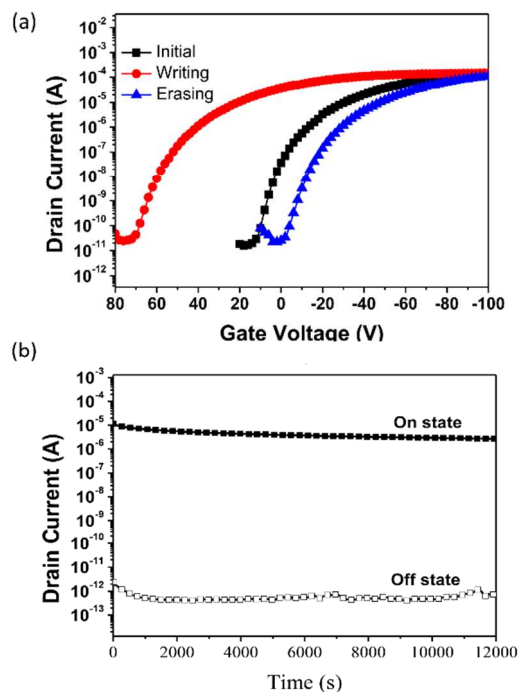


Fig. 2. (a) Shifts in transfer curves for pentacene OFET memory device with P4VP(2-Hydroxyanthracene)<sub>1</sub>. (b) Retention time of the P4VP(2-naphthol)<sub>1</sub>-based device.

Table 1. Characteristics of pentacene based OFET memory devices with supramolecular electrets

Small molecule	ratio	$\mu$ ( $\text{cm}^2\text{V}^{-1}\text{s}^{-1}$ )	On/Off <sup>[a]</sup>	$\Delta V_{\text{Th}}$ <sup>[b]</sup> (V)
Phenol	1:0.3	0.21	$3.8 \times 10^7$	11
	1:0.5	0.19	$3.2 \times 10^7$	27
	1:1	0.16	$2.9 \times 10^7$	43
2-Naphthol	1:0.3	0.20	$5.5 \times 10^7$	29
	1:0.5	0.26	$7.1 \times 10^7$	47
	1:1	0.23	$6.2 \times 10^7$	61
2-Hydroxyanthracene	1:0.3	0.17	$2.1 \times 10^7$	52
	1:0.5	0.16	$1.5 \times 10^7$	61
	1:1	0.12	$1.1 \times 10^7$	76

<sup>[a]</sup> On/off drain current ratios of reading at  $V_g = 0$  V. <sup>[b]</sup>  $\Delta V_{\text{Th}}$  is defined as  $V_{\text{Th(erasing)}} - V_{\text{Th(writing)}}$ .

The conjugation length of the electret may affect the memory window significantly. Table 1 and Figure S6 (SI) shows the memory windows of the pentacene based OFET memory devices on different polymer electrets, P4VP(2-Hydroxyanthracene)<sub>1</sub>, P4VP(2-Naphthol)<sub>1</sub> and P4VP(Phenol)<sub>1</sub>. The order of the  $V_{\text{Th}}$  shift at the devices is P4VP(2-Hydroxyanthracene)<sub>1</sub> > P4VP(2-Naphthol)<sub>1</sub> > P4VP(Phenol)<sub>1</sub>. It suggests the  $\pi$ -conjugation length enhance the memory window significantly. The LUMO levels of phenol, 2-naphthanol and 2-hydroxyanthracene are -0.01, -0.95 and -1.6 eV (Figure S7, SI), respectively, indicating that the longer conjugation length enhances electron affinity. When applying a positive gate bias, electrons tend to accumulate at the semiconductor/dielectric interface. Due to the external electric field, the electrons overcome the LUMO energy barrier between pentacene (-2.9 eV) and the tunnelling layer, P4VP (-0.54 eV), and sequentially transfer to the small molecules. Therefore, the low-lying LUMO level of the small molecules possess stronger electron affinity to drive the electron transfer, then leading to the increased amount of trapped charges. The above result suggests a simple methodology to tune the transistor memory characteristics through conjugated length of the electret. Note that the LUMO level of phenol is slightly higher than P4VP, but the memory device was still able to exhibit charge storage ability. It may be attributed to the formation of hydrogen bonding, facilitating the stabilization of trapped charges.

The time during which the stored charge is retained in the dielectric layer is defined as the retention time, as shown in Figure 2b. The charge retention time of the pentacene on P4VP(2-Hydroxyanthracene)<sub>1</sub>, P4VP(2-Naphthol)<sub>1</sub> and P4VP(Phenol)<sub>1</sub> electrets were monitored (Figure S8, SI). The retention time of the ON and OFF states of the device at a gate voltage of 0 V are maintained for  $10^4$  s. Note that, the P4VP(2-Naphthol)<sub>1</sub> device shows superior stability and highest on/off current ratio of around  $10^7$  (Table 1 and Figure 2b). The higher on/off ratio is mainly attributed to its highest hole mobility ( $0.23 \text{ cm}^2/\text{Vs}$ ), resulting in a larger ON-state current, and a stable charge trapping capability, which leads to a stable low OFF-state current. The multiple switching stability of the P4VP(2-Naphthol)<sub>1</sub> device was evaluated through write-read-erase-read (WRER) cycles (Figure S9, SI). The operation conditions of WRER cycles are summarized as the following. The drain current was measured at  $V_d = 100$  V. The writing, reading and erasing were at the gate voltages of -80, 0 and 80 V, respectively. The responding ON and OFF current of the device could be maintained over 100 cycles. The good stability and

reversibility suggested the potential applications using organic semiconducting nanowires for non-volatile flash-type memories.

## Conclusions

A simple method to prepare supramolecular thin film electrets is developed for non-volatile pentacene-based OFET memories with high performance. The intermolecular hydrogen-bonding interaction between P4VP and small molecules is confirmed by FTIR experiment. Quantitative analysis of the FTIR results reveals that at  $x < \sim 0.60$  almost all of the added small molecules are hydrogen bonded to the P4VP chains. The hydrogen bonding becomes incomplete when  $x$  exceeds 0.60 and saturates at  $x > 0.90$ . Besides, the effect of the molar ratio and conjugation lengths of electrets on OFET memory performance were revealed. The pentacene OFET memory device based on P4VP(2-hydroxyanthracene)<sub>1</sub> polymer electret exhibited the largest memory window (76V). This clearly indicates that the magnitude of memory windows is related to the fraction of the hydrogen-bonded benzene rings and conjugated lengths. Furthermore, the memory devices with P4VP(2-naphthol)<sub>1</sub> as electret exhibited high ON/OFF ratio of  $10^7$  and the ON or OFF state could be retained over  $10^4$  s. This study reveals a promising method to fabricate supramolecular electrets of memory device elements and analyse the memory properties of those devices with different supramolecular electrets.

## Notes and references

<sup>a</sup> Department of Chemical Engineering, National Taiwan University, Taipei 10617, Taiwan. E-mail: chenwc@ntu.edu.tw

<sup>†</sup> Electronic Supplementary Information (ESI) available: [FTIR spectra, AFM images, I-V curves and TEM images]. See DOI: 10.1039/c000000x/

- (a) Y. Guo, G. Yu and Y. Liu, *Adv. Mater.*, 2010, **22**, 4427-4447; (b) Q.-D. Ling, D.-J. Liaw, C. Zhu, D. S.-H. Chan, E.-T. Kang and K.-G. Neoh, *Prog. Polym. Sci.*, 2008, **33**, 917-978; (c) P. Heremans, G. H. Gelinck, R. Müller, K.-J. Baeg, D.-Y. Kim and Y.-Y. Noh, *Chem. Mater.*, 2010, **23**, 341-358; (d) C.-L. Liu and W.-C. Chen, *Polym. Chem.*, 2011, **2**, 2169-2174; (e) Y.-K. Fang, C.-L. Liu, C. Li, C.-J. Lin, R. Mezzenga and W.-C. Chen, *Adv. Funct. Mater.*, 2010, **20**, 3012-3024.
- (a) K. J. Baeg, Y. Y. Noh, J. Ghim, S. J. Kang, H. Lee and D. Y. Kim, *Adv. Mater.*, 2006, **18**, 3179-3183; (b) H. E. Katz, X. M. Hong, A. Dodabalapur and R. Sarpeshkar, *J. Appl. Phys.*, 2002, **91**, 1572-1576; (c) K.-J. Baeg, Y.-Y. Noh, J. Ghim, B. Lim and D.-Y. Kim, *Adv. Funct. Mater.*, 2008, **18**, 3678-3685; (d) J.-C. Hsu, W.-Y. Lee, H.-C. Wu, K. Sugiyama, A. Hirao and W.-C. Chen, *J. Mater. Chem.*, 2012, **22**, 5820-5827; (e) Y.-C. Chiu, I. Otsuka, S. Halila, R. Borsali and W.-C. Chen, *Adv. Funct. Mater.*, 2014, **24**, 4198-4198.
- (a) R. Schroeder, L. A. Majewski and M. Grell, *Adv. Mater.*, 2004, **16**, 633-636; (b) R. C. G. Naber, C. Tanase, P. W. M. Blom, G. H. Gelinck, A. W. Marsman, F. J. Touwslager, S. Setayesh and D. M. de Leeuw, *Nat Mater*, 2005, **4**, 243-248.
- (a) Y.-H. Chou, N.-H. You, T. Kurosawa, W.-Y. Lee, T. Higashihara, M. Ueda and W.-C. Chen, *Macromolecules*, 2012, **45**, 6946-6956; (b) Y.-H. Chou, H.-J. Yen, C.-L. Tsai, W.-Y. Lee, G.-S. Liou and W.-C. Chen, *J. Mater. Chem. C*, 2013, **1**, 3235-3243.
- (a) T. Sekitani, T. Yokota, U. Zschieschang, H. Klauk, S. Bauer, K. Takeuchi, M. Takamiya, T. Sakurai and T. Someya, *Science*, 2009, **326**, 1516-1519; (b) K.-J. Baeg, Y.-Y. Noh, H. Sirringhaus and D.-Y. Kim, *Adv. Funct. Mater.*, 2010, **20**, 224-230
- Y.-H. Chou, Y.-C. Chiu and W.-C. Chen, *Chem. Commun.*, 2014, **50**, 3217-3219.
- (a) S.-H. Tung, N. C. Kalarickal, J. W. Mays and T. Xu, *Macromolecules*, 2008, **41**, 6453-6462; (b) B. J. Rancatore, C. E. Mauldin, S.-H. Tung, C. Wang, A. Hexemer, J. Strzalka, J. M. J. Fréchet and T. Xu, *ACS Nano*, 2010, **4**, 2721-2729; (c) S.-J. Wang,

Y.-S. Xu, S. Yang and E.-Q. Chen, *Macromolecules*, 2012, **45**, 8760-8769.